PCCP
Physical Chemistry Chemical Physics

Accepted Manuscript

This article can be cited before page numbers have been issued, to do this please use: B. Yoon and G. S. Hwang, *Phys. Chem. Chem. Phys.*, 2020, DOI: 10.1039/D0CP02178D.

ROYAL SOCIETY OF CHEMISTRY

rsc.li/pccp

View Article Online
DOI: 10.1039/D0CP02178D

On the Mechanism of Predominant Urea Formation from Thermal Degradation of CO_2-loaded Aqueous Ethylenediamine

*Bohak Yoon and Gyeong S. Hwang**

McKetta Department of Chemical Engineering, University of Texas at Austin, Austin, Texas 78712, USA

This study attempts to explain the well-known experimental observation that 1,3-Bis(2-aminoethyl)urea (urea) is preferentially formed over the other major product, 2-imidazolidone (IZD), from thermal degradation of aqueous ethylenediamine (EDA) during the CO_2 capture process. This is in direct contrast to the case of monoethanolamine (MEA), preferentially forming oxazolidinone (OZD), rather than urea, which undergoes further reactions leading to more stable products. Given their similar molecular structures, the different preferred degradation pathways of EDA and MEA impose an intriguing question regarding the underlying mechanism responsible for the distinct difference. Thermal degradation of both EDA and MEA tends to proceed mainly via formation of isocyanate intermediate that may further undergo either cyclization to IZD (or OZD) or a reaction with EDA (or MEA) forming urea. For the EDA case, our first-principles simulations clearly demonstrate that the urea formation reaction is kinetically more, but thermodynamically less, favorable than the cyclization reaction; the opposite is true for the MEA case. Our further analysis shows that EDA-isocyanate is less prone to cyclization than MEA-isocyanate, which in turn allows for more facile urea formation. The reconfiguration dynamics of isocyanate is found to be governed by the dynamic nature of the interaction between its terminal group and surrounding solvent molecules. Our work highlights the importance of kinetic effects associated with the local structure and dynamics of solvent molecules around the intermediates that may significantly alter the degradation process of amine solvents.

*Author to whom correspondence should be addressed:

Tel: 1-512-471-4847, Fax: 1-512-471-7060, E-mail: gshwang@che.utexas.edu

Keywords: ethylenediamine, thermal degradation, entropic effects, CO_2 capture, ab initio molecular dynamics, metadynamics

View Article Online
DOI: 10.1039/D0CP02178D

TABLE OF CONTENTS

Urea formation is kinetically more favorable than IZD formation from thermal degradation of aqueous EDA during the CO_2 capture process.

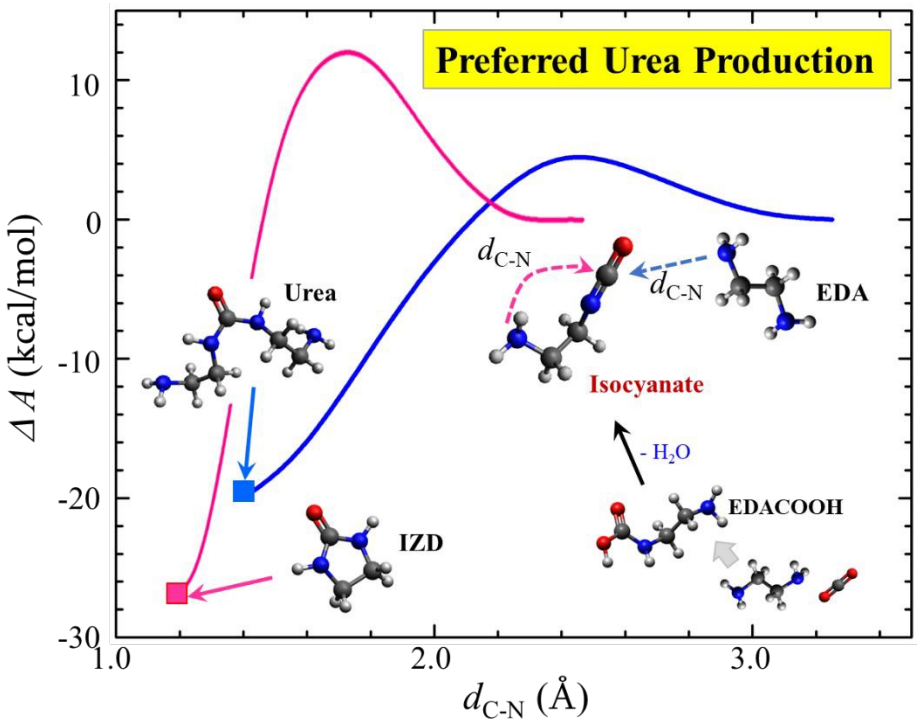

View Article Online
DOI: 10.1039/D0CP02178D

1. Introduction

Amine scrubbing using aqueous amine solutions remains to be the most efficient near-term solution for post-combustion CO_2 capture from flue gas at coal-fired power plants.[1,2] Monoethanolamine (MEA) is one of the most extensively tested alkanolamines, but its commercial application tends to be limited because of degradation and corrosion issues and enormous energy requirement for solvent regeneration.[3–6] About (~10 %) of total capital cost of CO_2 capture is attributed to makeup of amine solvent loss.[7–10] Moreover, some degradation products are considered to be dangerous if exposed to the environment.

Ethylenediamine (EDA) has been reported to have several advantages over MEA for its higher CO_2 capacity, faster CO_2 absorption rate, easier producible implementation from renewable resources, and slightly lower degradation rates at moderate CO_2 loading.[11–16] EDA contains two primary amine groups and MEA has one primary amine and one hydroxyl group, while the two end groups are separated by two -CH_2- groups in both molecules. Despite their structural similarity, the major thermal degradation products of CO_2-loaded EDA and MEA solutions have been found to be distinctly different.[11,17]

Thermal degradation of amines is generally understood to occur predominantly in the stripper due to high temperature (~ 100 - 120 ^oC) and is likely to increase with CO_2 loading.[18] Previous experimental studies proposed that thermal degradation of primary and secondary amines would be initiated by polymerization of carbamates, which can ultimately degrade to urea and imidazolidinones.[19,20] The MEA degradation is thought to proceed via 2-oxazolidinone (OZD) formation that may undergo further reaction with amines to form more stable products.[21] Our previous study predicted isocyanate formation

View Article Online
DOI: 10.1039/D0CP02178D

from dehydration of carbamic acid to be highly probable, and also showed that cyclization of intermediate isocyanate to OZD would be kinetically more facile than reaction with MEA to form urea in aqueous MEA solution. The formation of isocyanate, albeit very small quantity, has also been experimentally reported.[22,23] In contrast to the case of MEA, the major thermal degradation products of EDA have been identified to be 1,3-Bis(2-aminoethyl)urea and 2-imidazolidone from mass spectrometry and high performance liquid chromatography measurements, while urea formation appears to be preferred.[11,17]

In this work, we investigate molecular mechanisms underlying thermal degradation of EDA in CO_2-loaded solution, with particular focus on the underlying reason for the preferential formation of urea, rather than cyclic compounds, in contrast to the case of MEA. First, quantum mechanical calculations with an implicit solvent model are used to evaluate the thermodynamic favorability of previously proposed reaction pathways, including the relative stabilities of intermediates and products. Then, *ab initio* molecular dynamics (AIMD) simulations combined with metadynamics are performed to determine free-energy barriers for key elementary reactions involved in the EDA degradation. These results help to identify a preferred degradation pathway. Finally, we provide an explanation as to why EDA and MEA show different degradation behaviors based on further analysis of the interactions between intermediate isocyanate and surrounding solvent molecules.

2. Computational Methods

Implicit-solvent quantum mechanical (QM) calculations with the Gaussian 16 suite of programs[24] were performed at the B3LYP/6-311++G(d,p) level of theory.[25] The solvation model based on density (SMD) implicit solvation model developed by Truhlar and co-

View Article Online
DOI: 10.1039/D0CP02178D

workers[26] was used to predict the solvation enthalpies and free energies of all species examined. The vibrational contributions to the free energy were assessed through the harmonic frequency analysis. These computational methods, as also discussed in our previous studies,[27] have been demonstrated to be suitable for the case of CO_2-loaded aqueous amine solution.

Density functional theory (DFT)-based *ab initio* molecular dynamics (AIMD) simulations were performed using the Vienna Ab initio Simulation Package (VASP)[28] and the CPMD code[29]. The generalized gradient approximation (GGA) functionals of Perdew, Berke and Ernzerhof (PBE)[30] and revised PBE[31] were used in VASP and CPMD, respectively. We also confirmed that the choice of functional does not change the conclusions drawn based on the results (further discussion regarding this can be found in the Supporting Information). The projector augmented wave (PAW) method[32] (Troullier-Martins pseudopotentials[33]) was used to describe the interaction between the core and valence electrons; a planewave basis set with a kinetic energy cutoff of E_{cut} = 400 eV (540 eV) was employed in VASP (CPMD). Grimme's D3 correction (DFT-D3)[34] was implemented to describe the van der Waals interaction; this correction is known to alleviate the excess ordering of liquid structure and significantly improve liquid-state of water.[35] To integrate the equations of motion, a timestep of 1.0 fs (0.17 fs) was used in VASP (CPMD). We sampled the Brillouin zone using only the gamma point, due the lack of symmetry and structure in aqueous solutions studied. The convergence of the results was carefully checked with respect to E_{cut} and *k*-point sampling (see Supporting Information). We used a fictitious electron mass of 650 a.u. for CPMD; to ensure adiabaticity, we replaced all

View Article Online
DOI: 10.1039/D0CP02178D

hydrogen atoms by deuterium. For the free-energy calculations, we used metadynamics employing the well-tempered algorithm via the PLUMED package[36] within the CPMD code. During production runs, Gaussian hills with an initial hill height of 1.004 kcal/mol and a width of 0.05 Å were deposited at a rate of 10^{-4} fs^{-1} with the height decay set by a ΔT = 3000 K. A more detailed information regarding convergence of well-tempered metadyanmics runs and veracity of associated transition state can be found in the Supporting Information.

3. Results and Discussion

3.1. Thermodynamic evaluation of EDA degradation pathways

Based on existing experimental observations and our calculation results reported herein, as illustrated in Figure 1, we propose probable thermal degradation routes of aqueous EDA during CO_2 capture process, involving:

- EDA may react with CO_2 to form carbamate while releasing a proton from the EDA-CO_2 zwitterion. Then, the released proton is abstracted by O of carbamate to form carbamic acid, i.e., EDA + CO_2 → EDACOOH **(R1)** or N of NH_2 of nearby EDA to form protonated EDA, i.e., 2 EDA + CO_2 → $EDACOO^-$ + $EDAH^+$ **(R2)**.
- Carbamic acid may undergo dehydration to form isocyanate intermediate, i.e., EDACOOH → isocyanate + H_2O **(R3)**, as shown in our previous work on MEA, in which isocyanate could be a short-lived intermediate progressing to urea or IZD in an aqueous EDA solution.[11,23,37] The isocyanate may subsequently undergo the intramolecular ring-closure reaction forming IZD, i.e., isocyanate → IZD **(R4)** or may

View Article Online
DOI: 10.1039/D0CP02178D

react with nearby EDA to form urea, i.e., isocyanate + EDA → urea **(R5)**.

- Carbamic acid may directly react with nearby EDA with dehydration to form urea, i.e., EDACOOH + EDA → urea + H_2O **(R6)**.

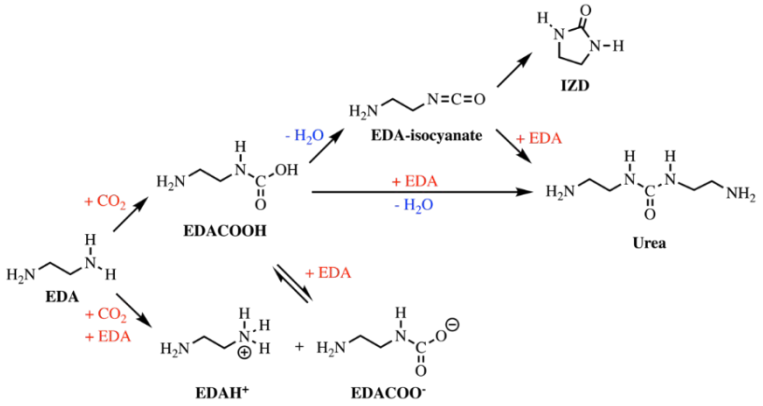

Figure 1. Proposed pathways for thermal degradation of aqueous ethylenediamine (EDA) solution in the CO_2 capture process.

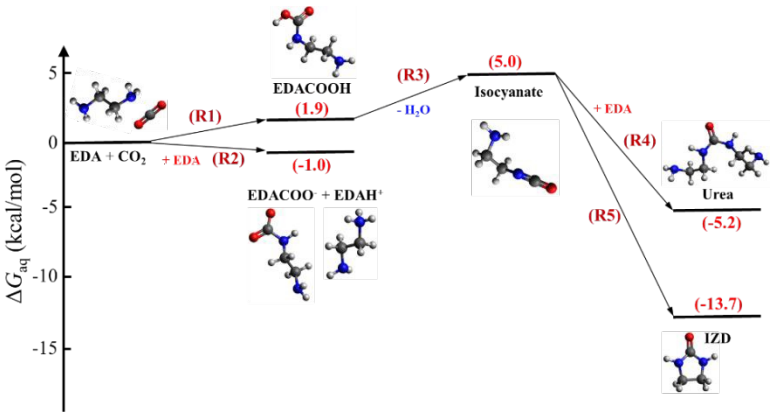

Figure 2. Predicted Gibbs free energy changes (ΔG_{aq}) for the elementary reactions involved in ethylenediamine (EDA) degradation in aqueous solution. Isolated EDA and CO_2 in aqueous solution are chosen as reference.

Figure 2 shows the change in Gibbs free energy (ΔG_{aq}) for each proposed reaction in aqueous solution, estimated using implicit solvent QM calculations. The EDA + CO_2 →

View Article Online
DOI: 10.1039/D0CP02178D

EDACOOH reaction **(R1)** is predicted to be slightly endergonic while the 2 EDA + CO_2 → $EDACOO^-$ + $EDAH^+$ reaction (**R2**) is exergonic by -1.0 kcal/mol. The thermodynamically preferred formation of $EDACOO^-/EDAH^+$ **(R2)** over EDACOOH **(R1)** can be understood by the chemical intuition that a primary amine is more basic than a carbamate.[38] Hence, in perspective of thermodynamics, the proton would favorably remain bonded to N in EDA to form the $EDACOO^-/EDAH^+$ pair in aqueous solution, instead of O of carbamate to form EDACOOH. Nonetheless, EDACOOH formation is also expected to be substantial at high CO_2 loadings in the stripper where the concentration of $EDACOO^-$ is much higher than that of free EDA at dynamic equilibrium. Moreover, the relative thermodynamic favorability of **R1** and **R2** depends on local environment. For instance, in the gas phase, ΔG_{gas} for **R2** is predicted to be much higher (≈ 137.0 kcal/mol) relative to that (≈ 16.91 kcal/mol) for **R1** (see Supporting Information for further details). This is expectable considering that the formation of charged $EDACOO^-/EDAH^+$ pair becomes far less energetically favorable than that of neutral carbamic acid in the gas phase. This implies that EDACOOH formation could be highly probable at stripper conditions in which water vaporization may lead to possible lack of stabilization of $EDACOO^-/EDAH^+$, especially when CO_2 loading is still relatively high. A similar behavior has been predicted in CO_2 capture by water-lean solvents.[39]

The formation of isocyanate from EDACOOH dehydration **(R3)** is predicted to be endergonic by 3.1 kcal/mol. Our previous study demonstrates that the isocyanate can be

View Article Online
DOI: 10.1039/D0CP02178D

fairly stable against rehydration and an important intermediate in the formation of degradation products.[27] The further reaction of isocyanate may lead to IZD (**R4**) or urea (**R5**). ΔG_{aq} are predicted to be -18.8 kcal/mol and -10.3 kcal/mol for **R4** and **R5**, respectively, suggesting that IZD formation is thermodynamically far more favorable than urea formation. The thermodynamic favorability of **R4** over **R5** contradicts the experimental observations that urea is a major, and IZD is a minor thermal degradation product. This analysis clearly demonstrates that thermal degradation of CO_2-loaded aqueous EDA solution cannot solely be explained by thermodynamics, suggesting that kinetics may play a key role in determining the major degradation product. In fact, it has been shown that the prevailing pathways for CO_2 capture and degradation in aqueous amine solutions are often governed by the relative rates of competing reactions, rather than the relative stabilities of intermediates and/or products.

In the following sections, we will evaluate free-energy barriers for elementary reactions involved in the thermal degradation of EDA, including EDACOOH dehydration, IZD formation via isocyanate cyclization, and urea formation involving isocyanate or EDACOOH.

3.2. Isocyanate *vs*. urea formation from EDACOOH

We first examined the mechanism of EDACOOH dehydration to form an isocyanate intermediate, in comparison to EDACOOH reaction with nearby EDA to form a urea. Thereafter, we also evaluated the stability of isocyanate towards (i) reaction with EDA to form urea, (ii) cyclization to form IZD, and (iii) rehydration back to carbamic acid. CPMD-

View Article Online
DOI: 10.1039/D0CP02178D

metadynamics simulations were performed at 313 K to determine the reaction pathway and associated free-energy barrier for EDACOOH dehydration in aqueous solution. 30 H_2O, 1 EDACOOH, and 1 EDA molecules are placed in a cubic simulation box of side length 10.4 Å with periodic boundary conditions, corresponding to about 19 wt% aqueous EDA solution at 0.5 CO_2 loading. As shown in Figure 3, the reaction pathway can be described by proton release from NH of EDACOOH, while the released proton is abstracted by the hydroxyl group of -COOH to form H_2O. In the metadynamics simulations, two collective variables (CVs) are employed: (i) the distance between N and H ($d_{N\text{-}H}$), representing the proton release from N in carbamic acid and (ii) $d_{O\text{-}HW} - d_{C\text{-}O}$, where $d_{O\text{-}HW}$ is the distance between the hydroxyl O in -COOH and the nearest H of H_2O, and $d_{C\text{-}O}$ is the distance between the carbonyl C and hydroxyl O atoms in -COOH, denoting the dehydration reaction. Here, a positive value represents the state prior to dehydration, i.e., EDACOOH; a negative value of $d_{O\text{-}HW} - d_{C\text{-}O}$ denotes the dehydrated state, i.e., isocyanate + H_2O.

Our CPMD-metadynamics simulations estimate $d_{N\text{-}H}$ = 0.98 Å, $d_{O\text{-}HW}$ = 2.23 Å, and $d_{C\text{-}O}$ = 1.42 Å at the initial state where the hydroxyl O of -COOH forms a hydrogen bond with H in neighboring H_2O, as illustrated in Figure 3. $d_{N\text{-}H}$ extends to 1.50 Å (indicating occurrence of deprotonation) while $d_{C\text{-}O}$ expands to 1.68 Å and $d_{O\text{-}HW}$ reduces to 1.14 Å at the transition state. At the final state, $d_{C\text{-}O}$ = 2.60 Å while $d_{O\text{-}HW}$ further decreases to 1.02 Å, representing the break of C-O bond and release of H_2O from EDACOOH leading to isocyanate formation; $d_{N\text{-}H}$ further increases to 2.73 Å (indicating completion of deprotonation). Evaluation of the free-energy surface indicates that the deprotonation from the N site may cause a weakening of the C-OH bond in -COOH, followed by C-OH bond

View Article Online
DOI: 10.1039/D0CP02178D

cleavage upon protonation of the hydroxyl O. The free-energy barrier for the dehydration reaction (**R3**) is estimated to be 27.8 kcal/mol, with a return barrier of 20.9 kcal/mol. Similar activation energies of 29.5 kcal/mol and 21.5 kcal/mol, respectively, are predicted from static QM calculations with implicit solvent (see Supporting Information). The dehydration behavior of EDACOOH is very similar to that of MEACOOH.[27]

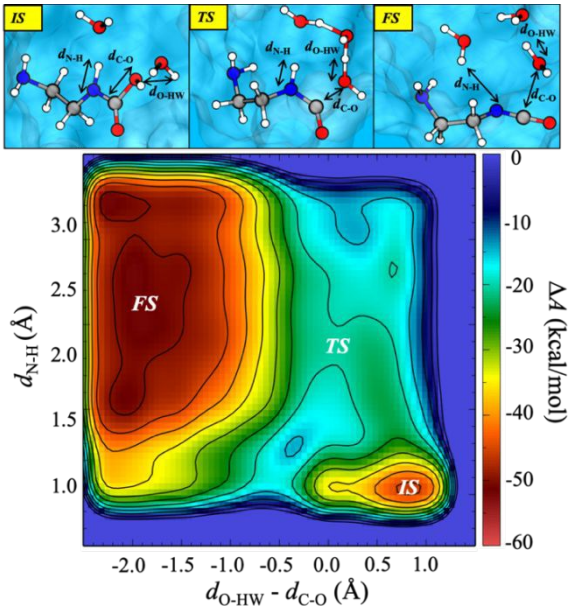

Figure 3. Free-energy surface (ΔA in kcal/mol) for dehydration of carbamic acid to isocyanate, i.e., EDACOOH $\rightarrow$ isocyanate + H_2O, predicted by CPMD-metadynamics simulations at 313 K. The positions of the initial (*IS*), transition (*TS*), and final (*FS*) states are denoted. Shown above are the corresponding molecular configurations, where the blue, red, grey, and white balls represent N, O, C, and H atoms, respectively.

The intermolecular reaction of EDACOOH with EDA accompanied by dehydration (**R6**), leading to urea formation, was also assessed using CPMD-metadynamics simulations at 313 K. As depicted in Figure 4, the basic N of the EDA may attack on the electrophilic carbonyl C of –COOH; this inclines to weaken the C-OH bond, followed by C-OH bond cleavage upon protonation of the hydroxyl O along with deprotonation of the terminal OH group. The metadynamics simulations employ two independent CVs; (i) the distance

View Article Online
DOI: 10.1039/D0CP02178D

between carbonyl C in -COOH and N of NH_2 in EDA ($d_{C\text{-}N}$), indicating the nucleophilic attack leading to C-N bond formation and (ii) $d_{C\text{-}O} - d_{O\text{-}HW}$, where $d_{C\text{-}O}$ is the distance between carbonyl C and hydroxyl O in -COOH, and $d_{O\text{-}HW}$ is the distance between hydroxyl O in -COOH and H in the nearest H_2O, representing the dehydration reaction. Here, a considerable negative value of $d_{C\text{-}O} - d_{O\text{-}HW}$ denotes the carbamic acid, i.e., EDACOOH + EDA, whereas a positive value indicates the state after dehydration, i.e., urea + H_2O. The estimated free-energy barrier for **R6** (direct urea formation) is about 31.3 kcal/mol, which is higher than that (= 27.8 kcal/mol) for **R3** (isocyanate formation). The difference in the energy barrier height would not be too considerable to completely disregard the intermolecular reaction especially at elevated temperatures. Nonetheless, our results clearly demonstrate the favorable production of isocyanate intermediate leading to IZD and urea formation.

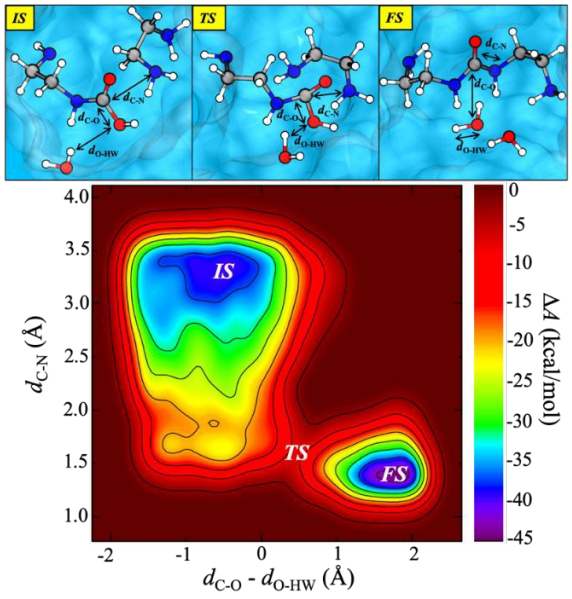

View Article Online
DOI: 10.1039/D0CP02178D

Figure 4. Free-energy surface (ΔA in kcal/mol) for reaction-dehydration of carbamic acid with EDA to urea, i.e., EDACOOH + EDA → urea + H_2O, predicted by CPMD-metadynamics simulations at 313 K. The positions of the initial (*IS*), transition (*TS*), and final (*FS*) states are indicated. Shown above are the corresponding molecular configurations, where the blue, red, grey, and white balls represent N, O, C, and H atoms, respectively.

3.3. Urea *vs*. IZD formation from isocyanate

We next evaluated the relative kinetic favorability of the two competing reactions of isocyanate to IZD (**R4**) and urea (**R5**), with comparison to isocyanate hydration to carbamic acid. Initially, standard AIMD simulations were performed to examine the possible conversion of isocyanate to IZD, urea and/or carbamic acid. The systems considered were similar to our previous studies on the MEA case.[27] 16 H_2O, 3 EDA, and 1 isocyanate, representing amine concentration of 42 wt%, were placed in a cubic simulation box of edge length 10.01 Å with periodic boundary conditions. The relatively high amine concentration compared to typical conditions (~ 30 wt%) was considered in order to speed up the possible intermolecular reaction between isocyanate and free amine in the limited simulation time span.[27]

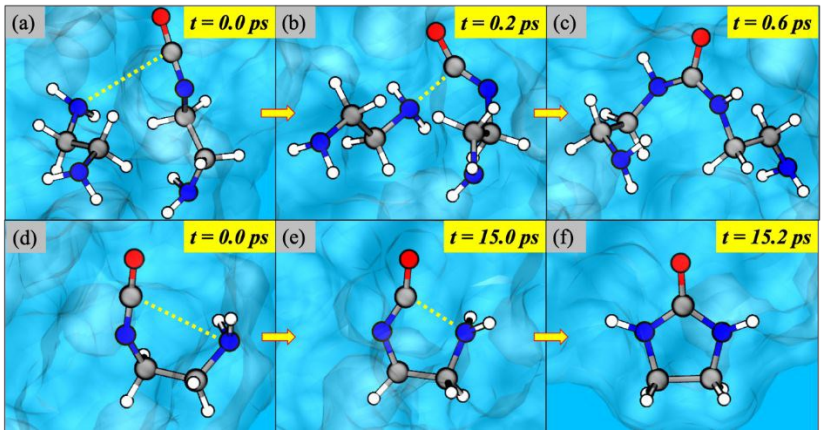

View Article Online
DOI: 10.1039/D0CP02178D

Figure 5. AIMD snapshots demonstrating reaction of isocyanate with EDA to urea (a-c) and ring-closure of isocyanate to IZD (d-f) both at 373 K. he blue, red, grey, and white balls represent N, O, C, and H atoms, respectively.

As shown in Figure 5, urea formation was observed from our AIMD simulations at 373 K. The electrophilic C in isocyanate is attacked by the nucleophilic N of nearby EDA [(a) → (b)], followed by proton transfer from the nucleophilic-attacking N of EDA to N in isocyanate [(b) → (c)] via a Grotthuss-like mechanism. We also observed IZD formation involving intramolecular cyclization [(d) → (e)] and subsequent proton transfer from N in the terminal group to N in the isocyanate group [(e) → (f)]. According to our AIMD simulations at 373 K, the IZD formation reaction generally tends to occur much more slowly than the urea formation reaction, implying that the latter would be kinetically more facile. Hydration of isocyanate to carbamic acid, following the reverse pathway for carbamic acid dehydration to isocyanate, was observed only at very high temperatures (~ 1000 K, see Supporting Information); this may reiterate that isocyanate can be fairly

View Article Online
DOI: 10.1039/D0CP02178D

resistant to hydration and an important intermediate in the formation of urea and IZD.

Using CPMD-metadynamics simulations, we subsequently evaluated the free-energy barriers for the two competing urea and IZD formation reactions, with particular attention to entropic contributions. Here, 30 H_2O, 1 isocyanate, and 2 EDA molecules were placed in a cubic periodic box with side length 10.77 Å, corresponding to about 27 wt% aqueous EDA solution. For the urea formation reaction, we used the distance between electrophilic C of –N=C=O and N of nearest EDA as a CV ($d_{C\text{-}N}$). For the IZD formation reaction, we also used a single CV, $d_{C\text{-}N,ring}$, the distance between electrophilic C of –N=C=O and basic N in the terminal amine group. Since both reactions are mainly manipulated by the C-N bond formation, the sole CV, $d_{C\text{-}N}$ ($d_{C\text{-}N,ring}$), appears to be appropriate and sufficient to evaluate their free-energy barriers.

For the case of urea formation in Figure 6(a), the relatively large $d_{C\text{-}N}$ of 3.25 Å at the initial state implies a complete separation of the C and N atoms with no significant interaction. The bond lengths of C-O and C-N with 1.23 Å and 1.21 Å, respectively, in –N=C=O indicate their double bond character; due to high electronegativities of N and O relative to those of C, the isocyanate group may form two resonance structures i.e., $-N^{\delta-}-C^{\delta+}=O \leftrightarrow -N=C=O \leftrightarrow -N=C^{\delta+}-O^{\delta-}$. The positive character of C indicates its susceptibility to nucleophilic attack. As N of EDA gets closer to the electrophilic C site of isocyanate, the C-O and C-N bonds of isocyanate stretches; at the transition state where $d_{C\text{-}N}$ = 2.48 Å, their bond lengths increase to 1.35 Å while changing its linear structure to a bent

View Article Online
DOI: 10.1039/D0CP02178D

configuration. With further progress of the reaction to urea formation, a proton is transferred from N of EDA to N of isocyanate; at the final state ($d_{C\text{-}N}$ = 1.40 Å), the C-N bond of isocyanate further stretches to 1.52 Å, while the C-O bond reduces back to 1.22 Å. The free-energy barrier formation reaction for the urea is predicted to be 4.8 kcal/mol.

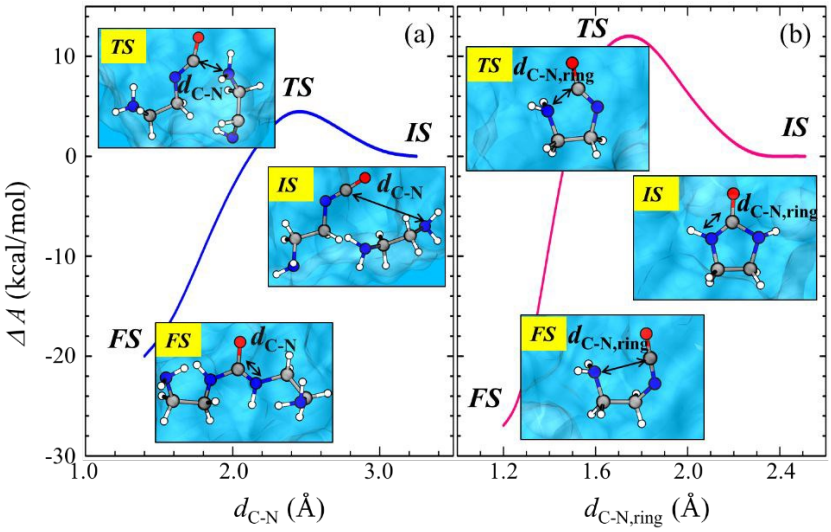

Figure 6. Free-energy surface (ΔA in kcal/mol) for (a) intermolecular reaction of isocyanate with EDA to form urea, and (b) intramolecular ring-closure of isocyanate to IZD, predicted by CPMD-metadynamics simulations at 313 K. Molecular configurations in the initial (*IS*), transition (*TS*), and final (*FS*) states are also shown; the blue, red, grey, and white balls represent N, O, C, and H atoms, respectively.

Following an analogous mechanism where N in the terminal amine group acts as a nucleophile, as shown in Figure 6(b), isocyanate cyclization to IZD is evaluated using CPMD-metadynamics simulations. At the initial state, $d_{C\text{-}N,ring}$ = 2.51 Å implies a negligible interaction between the C and N atoms. N in the terminal group undertakes nucleophilic addition to the C=N double bond of isocyanate. $d_{C\text{-}N,ring}$ are predicted to be 1.76 Å and 1.20 Å at the transition and final states, respectively. The predicted free-energy barriers for the IZD formation reaction is 12.1 kcal/mol, substantially higher than that (=

View Article Online
DOI: 10.1039/D0CP02178D

4.8 kcal/mol) for the urea formation reaction. We could attribute the relatively higher free-energy barrier for IZD formation largely to the tendency that reconfiguration of its chain-like structure is hindered due to the interaction between the terminal NH_2 and surrounding water molecules (*vide infra*).

We also performed CPMD-metadynamics simulations at 44 wt% amine concentration (16 water, 1 isocyanate, and 3 EDA molecules in a cubic periodic box with side length 9.77 Å) to further investigate how the free-energy barrier is influenced by the accessibility of the terminal NH_2 to –N=C=O. Our simulations predict a significant decrease (increase) in the barrier height to 2.7 (16.7) kcal/mol for the case of urea (IZD) formation. This is apparently due to the fact that the intermolecular interaction between isocyanate and EDA is enhanced by more populated EDA molecules surrounding the isocyanate, while the intramolecular cyclization of isocyanate becomes more hindered. This analysis also strongly indicates that the favorability of the competing reactions is largely determined by the relative rates of the intramolecular (ring closure) and intermolecular processes, which can further be a strong function of EDA concentration in aqueous solution.

In the following section, we attempt to identify the underlying mechanism responsible for the difference in the isocyanate reaction behavior in between aqueous MEA and EDA solutions.

3.4. What causes the difference between EDA and MEA decomposition pathways?

Comparing the molecular structures of EDA and MEA, the terminal hydroxyl group in MEA is replaced with an amine group in EDA, as illustrated in Figure 7. However, as pointed out earlier the major products of MEA thermal degradation are relatively large

View Article Online
DOI: 10.1039/D0CP02178D

diamine species formed via OZD (which tends primarily to result from isocyanate cyclization[27]). Our previous study highlights that the intramolecular cyclization reaction to OZD can be more facile than the intermolecular reaction between isocyanate and MEA forming urea, although the latter is thermodynamically more favorable than the former.[27] Under the nearly identical simulation conditions as the EDA case reported herein, the predicted free-energy barriers for the OZD and urea formation reactions are 5.1 and 15.1 kcal/mol, respectively.[27] Comparing with the EDA case (yielding 12.1 and 4.8 kcal/mol, respectively), the free-energy barrier for OZD formation is lower by 7 kcal/mol, whereas that for urea formation tends to increase greater than 10 kcal/mol. The distinct difference could be attributed to the entropic effects associated with the difference in the interaction of isocyanate with surrounding water molecules, as discussed in the following.

Given that the isocyanate cyclization reaction is initiated by the nucleophilic attack of the terminal base N (N_t) or O (O_t) atom, we examined the dynamics of its interaction with the isocyanate group C (C_i) atom by computing the radial distribution function (RDF) between the C_i and N_t (or O_t) atoms in aqueous solution using AIMD simulations at 313 K. The RDF is given by $g(r) = \langle n(r, r + dr)/4\pi r^2 \rho dr \rangle$, where $n(r, r + dr)$ is the number of C_i in a spherical shell of thickness dr and radius r (from the reference N_t or O_t) and ρ is the bulk number density. Each system contains 30 H_2O and 1 isocyanate molecules in a cubic periodic box of edge length 10.54 Å, and the $g(r)$ for each case was obtained from the average of 5 independent systems with different initial configurations.

View Article Online
DOI: 10.1039/D0CP02178D

As shown in Figure 7, the g(r) for the C_i-N_t pair exhibits a distinct sharp peak at about 4.6 Å, indicating that EDA-isocyanate may most probably exist in a linear-chain like configuration. On the other hand, the MEA case shows a broad g(r) profile ranging from 2 Å to 4.5 Å with a peak maximum at around 3 Å, implying that MEA-isocyanate would be more prone to cyclization than EDA-isocyanate. As detailed below, our further analysis suggests that the reconfiguration behavior can be strongly governed by the solvation dynamics of the terminal group.

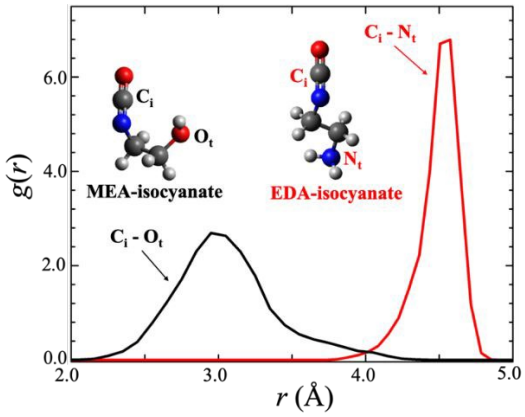

Figure 7. Radial distribution functions for the C_i-N_t pair in EDA-isocyanate (red solid line) and the C_i-O_t pair in MEA-isocyanate (black solid line) from AIMD simulations at 313 K. The blue, red, grey, and white balls in the isocyanate molecular structures shown represent N, O, C, and H atoms, respectively.

The structural and dynamical nature of the first hydration shell of the terminal hydroxyl and amine groups were investigated to clarify a possible correlation between the solvation and reconfiguration behaviors. Figure 8 shows g(r) for the hydrogen bonded pairs between the terminal groups and surrounding water molecules, as specified. In principle, the hydroxyl and amine groups may form the same number of hydrogen bonds (HBs), while

View Article Online
DOI: 10.1039/D0CP02178D

the former possess two HB acceptors and one donor and the latter has one HB acceptor and two donors. However, the areas under the first peak of g(r) to 2.6 Å for the N_t-H_w and O_t-H_w pairs give coordination numbers (CNs) of 1.0 and 1.7, respectively, while that for the H_t-O_w pair in each corresponding case gives a CN of either 1.4 or 1.0. The resulting total CNs of 2.4 and 2.7 indicate that the amine group forms slightly fewer HBs than the hydroxyl group, consistent with previous studies[40].

The RDF analysis also shows that the N_t atom is a stronger HB acceptor than the O_t atom, well demonstrated further by comparison of the N_t-H_w and O_t-H_w g(r) profiles in which the first peak near 1.7 Å for the N_t-H_w pair is sharper than that near 1.8 Å for the O_t-H_w pair. This is not surprising given that the amine N is more basic than the hydroxyl O, thereby having a stronger tendency to abstract a proton from water. Moreover, H_t in the amine group tends to be a much weaker HB donor than that in the hydroxyl group. Hence, a water molecule tends to be strongly bound to the N_t site.

The dynamics of the N_t-H_w and O_t-H_w HBs was further examined by calculating two distinct HB autocorrelation functions; (i) continuous HB correlation function $S(t)$ which depicts the probability that the initial HB between i and j pair molecules remains bonded at all times up to time t and (ii) intermittent HB correlation function $C(t)$ that describes the probability that of pair i and j molecules remaining hydrogen bonded at time t given that the pair was hydrogen-bonded at time 0 and is independent of the breaking of HBs at any intermediate time instant and allows for the re-formation of broken bonds. Figure 9 shows the corresponding average lifetimes, $\tau_{S,ij}$ and $\tau_{C,ij}$, representing the residence time of pair i and j molecules remain hydrogen bonded. The predicted $\tau_{S,ij}$ and $\tau_{C,ij}$ are 10.7 (1.8) and 18.7

View Article Online
DOI: 10.1039/D0CP02178D

(6.8) *ps*, respectively, for the HB between N_t (O_t) and H_W. The greater values of both $\tau_{S,ij}$ and $\tau_{C,ij}$ indicate the stronger binding of a water molecule to the N_t site than the O_t site. A more detailed description of the calculations can be found in the Supporting Information.

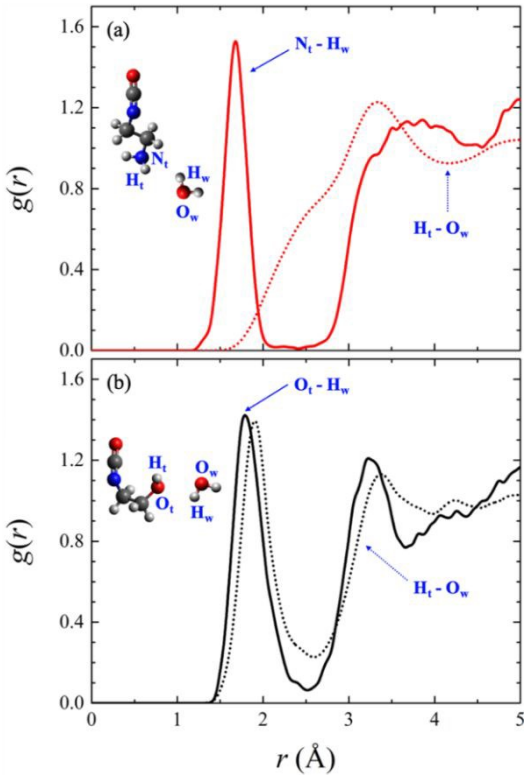

Figure 8. Radial distribution functions for (a) the N_t-H_w and H_t-O_w pairs in the EDA-isocyanate case and (b) the N_t-H_w and H_t-O_w pairs in the MEA-isocyanate case, as indicated, from AIMD simulations at 313 K. The blue, red, grey, and white balls in the molecular configurations shown represent N, O, C, and H atoms, respectively.

The strongly bound water molecule may suppress rearrangement of first-shell water molecules around the amine, as compared to the hydroxyl case. This is well supported by the analysis demonstrating that O atoms of the first-shell water molecules are more ordered around the amine than the hydroxyl.[41] The facile rearrangement of surrounding water molecules can allow the terminal hydroxyl group relatively easily to interact with the

View Article Online
DOI: 10.1039/D0CP02178D

isocyanate group (see Figure 7), thereby making MEA-isocyanate more prone to cyclization than EDA-isocyanate. Our work highlights that the reconfiguration dynamics of isocyanate intermediate can be strongly influenced by the dynamic nature of the interaction between its terminal group and surrounding solvent molecules.

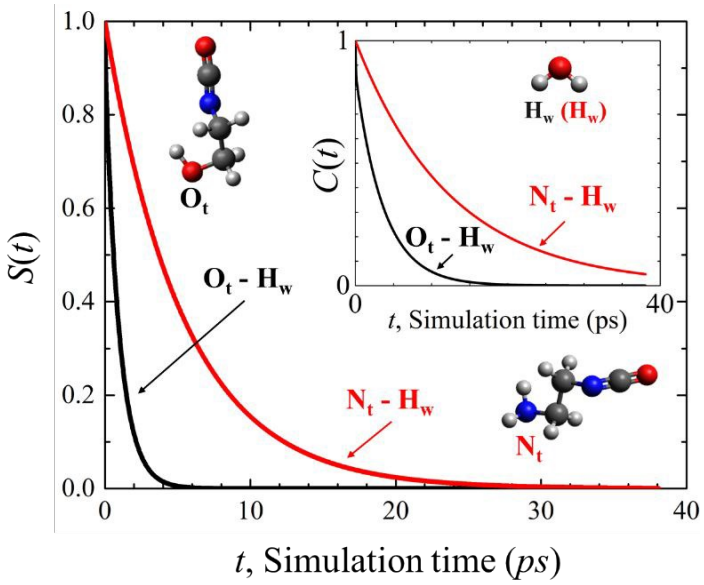

Figure 9. Continuous hydrogen bond autocorrelation functions for the N_t-H_w and O_t-H_w pairs, as indicated, from AIMD simulations at 313 K. Inset shows intermittent hydrogen bond autocorrelation functions for the same pairs. The blue, red, grey, and white balls in the molecular configurations shown represent N, O, C, and H atoms, respectively.

4. Summary

We have identified the underlying mechanism of predominant urea production from thermal degradation of CO_2-loaded EDA (ethylenediamine) solution by evaluating both thermodynamic and kinetic favorability of key elementary reactions involved. Our results clearly demonstrate that the preferred thermal degradation route of EDA is distinctly different from that of MEA (monoethanolamine), although they have structural similarity.

View Article Online
DOI: 10.1039/D0CP02178D

- Similar to the MEA case, the degradation of EDA is found to mainly proceed via formation of isocyanate intermediate by dehydration of carbamic acid. A carbamic acid may also react with EDA, followed by dehydration, to form urea; however, this reaction tends to be less kinetically favorable. The isocyanate may further undergo either cyclization to IZD (2-imidazolidone) or a reaction with EDA forming urea. For the case of MEA, the isocyanate cyclization results in OZD (oxazolidinone).
- Our CPMD-metadynamics simulations predict the free-energy barriers for the two competing IZD and urea formation reactions to be 12.1 and 4.8 kcal/mol, respectively, in about 27 wt% aqueous EDA solution. In contrast, for the MEA case, the predicted barrier for isocyanate cyclization (≈ 5.1 kcal/mol) is substantially lower than that for urea formation (≈ 15.1 kcal/mol). For both EDA and MEA cases, the intermolecular urea formation (intramolecular cyclization) reaction tends to be facilitated (suppressed) as the water content decreases. While the results clearly demonstrate the kinetic favorability of the urea formation reaction over the isocyanate cyclization to IZD, QM calculations with an implicit solvent model predict the former to be thermodynamically less favorable than the latter; however, the opposite is true for the case of MEA.
- Our further analysis demonstrates that EDA-isocyanate is less prone to cyclization than MEA-isocyanate, allowing for more facile nucleophilic attack of nearby EDA on the isocyanate responsible for the preferred urea formation. The reconfiguration dynamics of isocyanate intermediate is found to be strongly

View Article Online
DOI: 10.1039/D0CP02178D

influenced by the dynamic nature of the interaction between its terminal group, either hydroxyl (in MEA) or amine group (in EDA), and surrounding solvent molecules.

This work highlights that both kinetics and mechanisms of the reactions involved in thermal degradation may be largely determined by the entropic effects arising from changes in the dynamic nature of both intramolecular and intermolecular interactions. The enhanced fundamental understanding may aid efforts to minimize solvent degradation in the carbon capture process.

5. Acknowledgements

This work was supported by the Korea CCS R&D Center (KCRC) grant (No. 2015053544) funded by the Korea government (Ministry of Science, ICT & Future Planning) and the R.A. Welch Foundation (No. F-1535). We would like to thank the Texas Advanced Computing Center for use of the Stampede supercomputing system (OCI-1134872).

References

[1] G. T. Rochelle, *Science*, 2009, **325**, 1652–4.
[2] P. Luis, *Desalination*, 2016, **380**, 93–99.
[3] M. R. M. Abu-Zahra, L. H. J. Schneiders, J. P. M. Niederer, P. H. M. Feron and G. F. Versteeg, *Int. J. Greenh. Gas Control*, 2007, **1**, 37–46.
[4] M. R. M. Abu-Zahra, J. P. M. Niederer, P. H. M. Feron and G. F. Versteeg, *Int. J.*

View Article Online
DOI: 10.1039/D0CP02178D

Greenh. Gas Control, 2007, **1**, 135–142.
[5] D. M. D'Alessandro, B. Smit and J. R. Long, *Angew. Chem. Int. Ed. Engl.*, 2010, **49**, 6058–82.
[6] H. M. Stowe and G. S. Hwang, *Ind. Eng. Chem. Res.*, 2017, **56**, 6887–6899.
[7] A. B. Rao and E. S. Rubin, *Environ. Sci. Technol.*, 2002, **36**, 4467–4475.
[8] A. J. Reynolds, T. V. Verheyen, S. B. Adeloju, A. L. Chaffee and E. Meuleman, *Int. J. Greenh. Gas Control*, 2015.
[9] G. S. Goff and G. T. Rochelle, *Ind. Eng. Chem. Res.*, 2006, **45**, 2513–2521.
[10] S. A. Mazari, B. Si Ali, B. M. Jan, I. M. Saeed and S. Nizamuddin, *Int. J. Greenh. Gas Control*, 2015.
[11] S. Zhou, X. Chen, T. Nguyen, A. K. Voice and G. T. Rochelle, *ChemSusChem*, 2010, **3**, 913–918.
[12] M. Rabensteiner, G. Kinger, M. Koller, G. Gronald and C. Hochenauer, *Int. J. Greenh. Gas Control*, 2014, **27**, 1–14.
[13] S. Kadiwala, A. V. Rayer and A. Henni, *Chem. Eng. J.*, 2012, **179**, 262–271.
[14] J. Li, A. Henni and P. Tontiwachwuthikul, *Ind. Eng. Chem. Res.*, 2007, **46**, 4426–4434.
[15] Z. Wang, M. Fang, Y. Pan, S. Yan and Z. Luo, *Chem. Eng. Sci.*, 2013.
[16] A. P. Salvi, P. D. Vaidya and E. Y. Kenig, *Can. J. Chem. Eng.*, 2014, **92**, 2021–2028.
[17] J. Thompson, H. Richburg and K. Liu, in *Energy Procedia*, 2017.
[18] D. Hatchell, O. Namjoshi, K. Fischer and G. T. Rochelle, *Energy Procedia*, 2014, **63**, 1558–1568.
[19] H. Lepaumier, D. Picq and P. L. Carrette, in *Energy Procedia*, 2009.
[20] H. Lepaumier, E. F. Da Silva, A. Einbu, A. Grimstvedt, J. N. Knudsen, K. Zahlsen and H. F. Svendsen, in *Energy Procedia*, 2011.
[21] J. Davis and G. Rochelle, *Energy Procedia*, 2009, **1**, 327–333.
[22] T. Sakakura, J. C. Choi and H. Yasuda, *Chem. Rev.*, 2007, **107**, 2365–2387.
[23] T. E. Waldman and W. D. McGhee, *J. Chem. Soc. Chem. Commun.*, 1994, 957.
[24] M. J. Frisch, G. W. Trucks, H. B. Schlegel, G. E. Scuseria, M. A. Robb, J. R. Cheeseman, G. Scalmani, V. Barone, B. Mennucci, G. A. Petersson, H. Nakatsuji, M. Caricato, X. Li, H. P. Hratchian, A. F. Izmaylov, J. Bloino, G. Zheng, J. L. Sonnenberg, M. Hada, M. Ehara, K. Toyota, R. Fukuda, J. Hasegawa, M. Ishida, T. Nakajima, Y. Honda, O. Kitao, H. Nakai, T. Vreven, J. A. Montgomery, J. E. Peralta, F. Ogliaro, M. Bearpark, J. J. Heyd, E. Brothers, K. N. Kudin, V. N. Staroverov, T. Keith, R. Kobayashi, J. Normald, K. Raghavachari, A. Rendell, J. C. Burant, S. S. Iyengar, J. Tomasi, M. Cossi, N. Rega, J. M. Millam, M. Klene, J. E. Knox, J. B. Cross, V. Bakken, C. Adamo, J. Jaramillo, R. Gomperts, R. E. Stratmann, O. Yazyev, A. J. Austin, R. Cammi, C. Pomelli, J. W. Ochterski, R. L. Martin, K. Morokuma, V. G. Zakrzewski, G. A. Voth, P. Salvador, J. J. Dannenberg, S. Dapprich, A. D. Daniels, O. Farkas, J. B. Foresman, J. V. Ortiz, J. Cioslowski and D. J. Fox, *Gaussian09 Revis. C.01*, Gaussian, Inc., Wallingord CT, 2010.
[25] A. D. Becke, *J. Chem. Phys.*, 1993, **98**, 5648–5652.

View Article Online
DOI: 10.1039/D0CP02178D

[26] A. V Marenich, C. J. Cramer and D. G. Truhlar, *J. Phys. Chem. B*, 2009, **113**, 6378–6396.
[27] B. Yoon, H. M. Stowe and G. S. Hwang, *Phys. Chem. Chem. Phys.*, 2019.
[28] G. Kresse and J. Furthmuller, *Phys. Rev. B Condens. Matter Mater. Phys.*, 1996, **54**, 11169–11186.
[29] R. Car and M. Parrinello, *Phys. Rev. Lett.*, 1985, **55**, 2471–2474.
[30] J. P. Perdew, K. Burke and M. Ernzerhof, *Phys. Rev. Lett.*, 1996, **77**, 3865–3868.
[31] Y. Zhang and W. Yang, *Phys. Rev. Lett.*, 1998, **80**, 890.
[32] G. Kresse and D. Joubert, *Phys. Rev. B*, 1999, **59**, 1758–1775.
[33] N. Troullier and J. L. Martins, *Phys. Rev. B*, 1991, **43**, 8861–8869.
[34] L. Goerigk and S. Grimme, *Phys. Chem. Chem. Phys.*, 2011, **13**, 6670–6688.
[35] M. J. Gillan, D. Alfè and A. Michaelides, *J. Chem. Phys.*, 2016, **144**.
[36] M. Bonomi, D. Branduardi, G. Bussi, C. Camilloni, D. Provasi, P. Raiteri, D. Donadio, F. Marinelli, F. Pietrucci, R. A. Broglia and M. Parrinello, *Comput. Phys. Commun.*, 2009, **180**, 1961–1972.
[37] M. J. Horvath, D. Saylik, P. S. Elmes, W. R. Jackson, C. G. Lovel and K. Moody, *Tetrahedron Lett.*, 1999.
[38] H. M. Stowe, E. Paek and G. S. Hwang, *Phys. Chem. Chem. Phys.*, 2016, **18**, 25296–25307.
[39] Z. Bacsik, N. Ahlsten, A. Ziadi, G. Zhao, A. E. Garcia-Bennett, B. Martin-Matute and N. Hedin, *Langmuir*, 2011, **27**, 11118–11128.
[40] J. Hladílková, H. E. Fischer, P. Jungwirth and P. E. Mason, *J. Phys. Chem. B*, 2015, **119**, 6357–6365.